

The Space Clock PHARAO: Functioning and Expected Performances

Ph LAURENT^{1*}, A. CLAIRON¹, P. LEMONDE¹, G. SANTARELLI¹, C. SALOMON²,
C. SIRMAIN³, F. PICARD³, Ch. DELAROCHE³, O. GROSJEAN³, M. SACCOCCIO³, M. CHAUBET³, L.
GUILLIER³, J. ABADIE³,

1 BNM-SYRTE, 61 avenue de l'Observatoire, 75014 Paris, France

2 ENS-LKB, 24 rue Lhomond, 75231 Paris, France

3 CNES, 18 avenue Edouard Belin, 31401 Toulouse cedex, France

Abstract-The cold atom space clock PHARAO is one of the ultra-stable atomic clocks of the ESA supported ACES mission. ACES will fly on an external pallet of the European module Columbus of the International Space Station between mid 2006 and the end of 2007. The goal of PHARAO is the study and utilization of a laser cooled cesium clock in microgravity environment. The French space agency, CNES, is funding and managing the clock construction with the support of the BNM-SYRTE and LKB laboratories for the clock requirements and follow-up of subsystem development in industrial companies.

The clock sub-systems have been designed and the engineering models will be delivered in 2003 to the CNES technical center, in Toulouse, where the clock will be assembled, tested and evaluated.

In this paper, we present the PHARAO performances in term of frequency stability and accuracy and the technical solutions developed to reach these performances.

I. Introduction

PHARAO, as "Projet d'Horloge Atomique à Refroidissement d'Atomes en Orbite", has started in 1993 with the objective of performing Science with a space cold atom clock [1]. As a matter of fact, the combination of atomic laser cooling techniques [2] and microgravity environment allows the development of clocks with unprecedented performances. The frequency accuracy is expected to reach 10^{-16} or better.

To demonstrate the feasibility of a compact cold atom clock, BNM-SYRTE and LKB with the support of CNES have undertaken the construction of a clock prototype in 1994. The prototype was constructed and successfully tested in 1997 on board a zeroG aircraft [3]. This work has essentially brought on the volume reduction of the clock and on the improvement of the clock operation reliability with respect to the current atomic fountains. The objective was to show that current technologies were compatible with the requirements of the space development. On the same year, ESA, the European space agency, has accepted our proposal, ACES (Atomic Clock Ensemble in Space) [4], to make fundamental physics by using a cold atom clock, an H-maser and a time and frequency transfer package. The payload is to be flown on board the space station.

After leading the usual initial phase for the development of a space instrument, CNES has decided to fund the construction of the cold atom clock in 2001. The development philosophy is to subcontract the construction of the different clock sub-systems by some manufacturers. The cold atom clock includes 7 sub-systems. The clock will then be assembled, tested and validated at the CNES technical centre in Toulouse. In the current organization, CNES is the prime contractor and BNM-SYRTE and LKB are scientific and technical advisers.

EADS SODERN is developing the laser source and the cesium tube. The laser source provides all the laser tools for the atomic cooling, launching and detection. The cesium tube provides the atomic source, the controlled environment for the atomic manipulation. It receives, through optical fibers connected to the laser source, 10 laser beams; 6 are devoted to the cooling and the launching, 2 to the atomic internal state selection and 2 to the measurement of the atomic populations of the two hyperfine levels. The cesium tube also includes the interrogation Ramsey cavity which was constructed by THALES-TED.

The 9.2 GHz microwave signals are generated by a microwave source provided by THALES-TAS. The master oscillator is a quartz oscillator developed by CMAC.

All these sub-systems are controlled by a computer constructed by EREMS and a software package developed by CsSi. The computer also manages the data flux between the clock and the ACES payload.

The clock layout is represented on figure 1. The clock weighs 91 kg and fills a volume of about 200 l. The electric consumption is 114 W.

The space clock development includes the construction of two models of the clock. The assembly of the engineering model will begin in September 2003. It will be used to verify the interface compatibilities, the clock operation and its performances. Depending on the results, the design of the flight model could be slightly modified.

The space clock operation is similar to that of an atomic fountain. It operates sequentially by playing the same successive phases: atomic capture, launching, cooling, selection, microwave interrogation and detection by the atoms fluorescence induced by laser beams. The major differences arise from the one way atomic path inside the microwave

*e-mail: philippe.laurent@obspm.fr

cavity and from the possibility to vary the atomic velocity from 5 to 500 cm/s. The expected performances are a frequency stability of $10^{-13} t^{-1/2}$ and an accuracy of 10^{-16} .

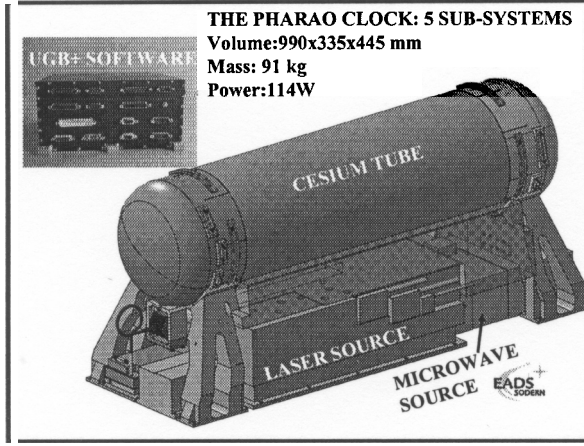


Fig. 1. Layout of the cold atom clock PHARAO for the ACES payload. The computer, UGB, will be placed on a vertical wall of the ACES pallet. (courtesy of EADS SODERN).

In the following, we will describe the technical solutions implemented to reach these performances. A first part deals with the short term frequency stability of the clock and the second deals with the long term frequency stability and accuracy. We end with a brief description of the main sub-systems of the clock

II. Short-term frequency stability

The short term frequency stability of a cold atom clock is described by the Allan variance given by :

$$\hat{\gamma}_y^2(\tau) = \left(\frac{\Delta\nu}{\bar{\omega}_\nu} \right)^2 \frac{T_c}{\tau} \left(\frac{1}{N_{at}} + \hat{\gamma}_{dl}^2 + \frac{2\hat{\gamma}_{SN}^2}{N_{at}^2} \right) + \frac{1}{\tau} \sum_{n=1}^{\infty} \frac{g_n^2}{g_0^2} S_y^{LO} \left(\frac{n}{T_c} \right)$$

Where $\Delta\nu$ is the atomic microwave resonance linewidth, ν is the microwave frequency (9,19... GHz), T_c is the cycle time and T the integration time.

Four main sources of noise contribute to the degradation the frequency stability: The first one is the quantum projection noise [5]. It varies as the inverse of the number of detected atoms, N_{at} . This term defines the ultimate limit of the clock frequency stability. The second and the third term bring together all the technical noises such as the detection laser noise (independent of the number of detected atoms) or the detection system noise. Finally, the fourth term results from the microwave signal frequency noise [6]. This noise level is mainly determined by the master quartz oscillator noise S_y^{LO} .

The g_n are the Fourier coefficients of the atomic sensitivity function during an operating cycle.

Projection noise

To minimize this term, the first precaution is to limit the loss of cold atoms during their flight between the capture region and the detection zone (see fig. 4). The geometry criteria are mainly defined by the microwave cavities apertures. For this space clock, we have designed a new Ramsey cavity geometry with large apertures (8x9mm) while keeping a low phase gradient on the internal microwave field. The resulting atomic losses obviously depend on the thermal expansion of the cold atom cloud. A slow decrease of the laser intensities is applied at the end of the cooling phase to reach a temperature of 1 μ K.

The collision losses with the background gas are reduced to less than a few per cent, whatever the atomic velocity, by maintaining a 10^{-8} Pa vacuum level. The outgassing of all materials has been measured and the fitted pumping system includes an ion pump and several getters. The ion pump is being space qualified. Another source of collisional losses comes from the Cs vapor escaping the capture zone. Graphite getters trap the major part and only a very low density collimated cesium beam along the cold atom path remains. The resulting cold atom losses are also less than a few percent.

To capture and cool a large number of atoms, while preserving a low density, we use the optical molasses configuration with six laser beams [7]. All 6 laser beams have a 13 mm beam waist radius and a 5.6 mW/cm² peak intensity. The cesium vapor pressure can be adjusted between $5 \cdot 10^{-7}$ to $5 \cdot 10^{-6}$ Pa to optimize the atom number. We expect to load a maximum of $1.5 \cdot 10^8$ atoms in 500ms ($1.5 \cdot 10^7$ atoms in $m_F=0$ sub-level). In fig. 2, we have represented the number of detected atoms and the projection noise contribution to the Allan standard deviation for a 1 s averaging time as a function of the atomic velocity. These results are obtained by simulating the cold atomic cloud behavior inside the cesium tube. With the previous parameters, the number of detected atoms varies from 3000 at 5 cm/s to $3 \cdot 10^6$ at 5m/s. The standard deviation remains below 10^{-13} for velocities between 15 to 150 cm/s. The optimal value, $7 \cdot 10^{-14}$, is obtained for a launching velocity of 50 cm/s.

Technical noise sources

The atoms are selectively detected by their fluorescence induced by 2 standing wave laser beams tuned to the $F=4$, $F'=5$ Cs line. Between the 2 beams, we have a pushing beam to remove the atoms in the $F=4$ level and a pumping beam to set the $F=3$ atoms in the $F=4$ state. The beams are slightly tilted with respect to the cesium tube axis. The residual cesium thermal beam is then Doppler-shifted and its contribution to stray fluorescence is reduced by an order of magnitude. Its contribution to the detection noise is negligible.

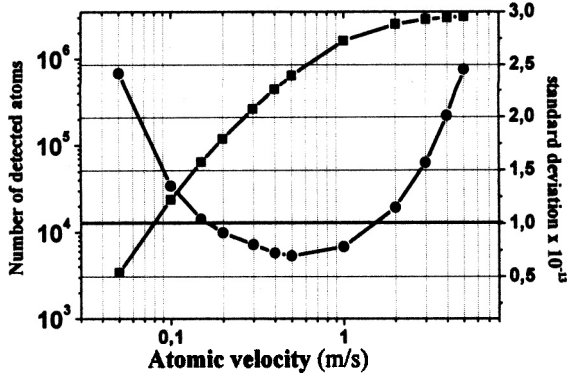


Fig. 2: Evolution of the number of detected atom (square) and of the resulting clock Allan standard deviation as a function of the atomic velocity. Only the projection noise is taken into account. The loading time is 500 ms.

The laser beam intensity and frequency noise are the main sources of noise on the atomic fluorescence fluorescence. These are made negligible as compared to the projection noise by the use of an extended cavity diode laser frequency servo-locked to a cesium line. We have developed a new ECDL concept [8] using an extended cavity closed by a semi-reflecting mirror and with an intra-cavity thin glass Fabry-Perot for the mode selection. The system has the advantage to be rugged and to operate in air or in vacuum on the same laser mode without any realignment. The servo-loop has a bandwidth of 30 kHz and the resulting frequency noise spectral density reaches $10^4 \text{ Hz}^2/\text{Hz}$ at 100 Hz. The laser intensity is also servo-locked by measuring the laser beam power inside the tube and by retro acting on an acousto-optic modulator of the laser source. The relative intensity noise is $2 \cdot 10^{-10}/\text{Hz}$ at 100 Hz. With these characteristics, the laser noise contributions are negligible with respect to the projection noise.

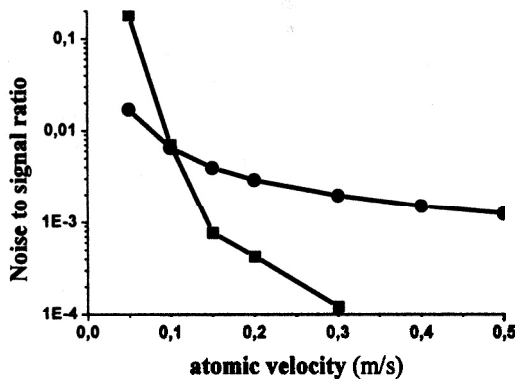


Figure 3 : contributions of the projection noise (circle) and the detection noise (square) to the detected noise to signal ratio. The atom number is shown in fig. 2.

The fluorescence detection efficiency is 5%. Several combinations of photodiode, amplifier and feedback resistance have been studied. The noise of the best system, when it is cooled to 15°C, is shown in figure 3. As compared to the projection noise, the detection noise becomes negligible for atomic velocity larger than 15 cm/s.

Quartz oscillator noise effect

Four state-of-the-art quartz oscillators have been space qualified for our application. An example of the measured frequency stability is shown in figure 4. These measurements have been obtained by comparing the quartz oscillator to a cryogenic sapphire oscillator from the University of Western Australia. The frequency stability reaches $6 \cdot 10^{-14}$. The stability is more or less constant from 1 to 10s integration time.

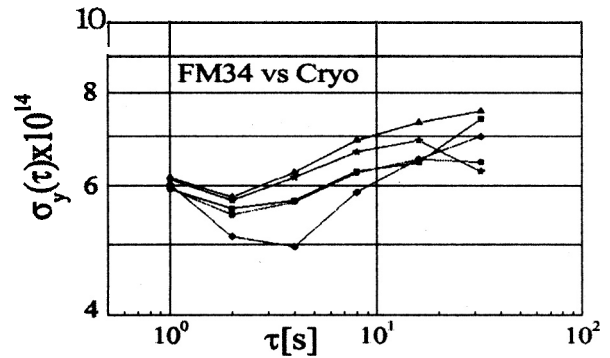


Figure 4: Measurements of the frequency stability of the quartz oscillator flight model.

Fig. 5 shows the simulations of the clock standard deviation. These results have been obtained by using the previous physical parameters and the measured phase noise of the quartz oscillator. The standard deviation is degraded for high velocities mainly due to the low duty cycle (the loading time is 500 ms, and the interrogation time is ~100ms). It remains below 10^{-13} for velocities lower than 1 m/s.

As a consequence of all noise sources, the frequency stability of the clock will be close to $10^{-13} t^{-1/2}$ for 30 to 50 cm/s atomic velocities.

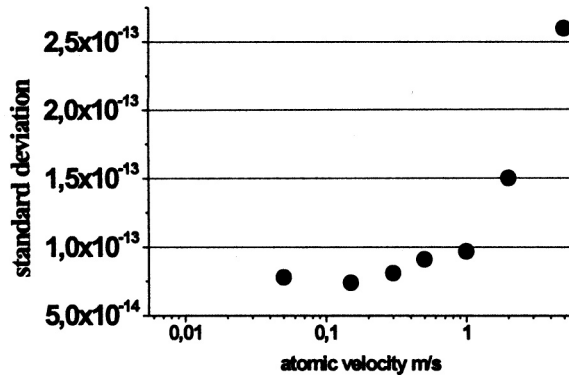


Fig. 5. Clock standard deviation as a function of the atomic velocity. The quartz noise oscillator is only taken into account.

III. Long term stability and accuracy

To prevent the magnetic environment effects, the cesium tube is protected by 3 cylindrical magnetic shields (figure 6). With a mock-up, we have measured a magnetic attenuation of about 10^5 . This is not enough to efficiently reduce the earth magnetic field modulation due to the rotation of the space station; the amplitude is about 25 μ T. An active servo-loop, including a probe and a solenoid inside the external shield, increases the attenuation by at least a factor of ten. The residual fluctuations will then remain below 20 pT.

Simulations of the magnetic field homogeneity along the atomic path show that, with 2 solenoids and 4 coils, the magnetic homogeneity inside the Ramsey cavity is smaller than 0.1 nT and the field gradients satisfy the adiabatic condition along the atomic path. The magnetic C-field can be adjusted from 10 nT to 1 μ T by varying the current inside the central solenoid. Besides, a degaussing system can be used during the mission. Maps of the magnetic field will be periodically performed with the atoms by means of pulses of sinusoidal current circulating inside a wire parallel to the atomic trajectory. The resulting magnetic field induces transitions between the atomic Zeeman sub-levels and a resonance signal can be detected after applying a resonant microwave pulse in the second interaction zone of the Ramsey cavity. The frequency stability and accuracy of the second order Zeeman effect will be a few 10^{-17} .

The interrogation zone is temperature regulated to within 0.1 K and with an absolute uncertainty of 0.2 K. All the temperature probes and their electronic commands have been characterized. Hence, the stability of the blackbody frequency shift will remain below $5 \cdot 10^{-17}$. Currently, the knowledge of this effect is still insufficient for an accuracy of 10^{-16} [9]. New measurements have then to be made, inside a fountain for instance, to go further.

To minimize the cold collisions, cold atoms are prepared in an optical molasses. The expected frequency shift ranges from 0.1 to $10 \cdot 10^{-15}$, depending on the atomic velocity (same loading time). The cold collision shift is a function of the time evolution of the atomic cloud and its study is based on the number of detected atoms through the fluorescence light. In the

clock, all physical parameters, cesium vapor pressure, laser intensities and frequencies,..., are controlled with a stability of 1%. Hence, the stability of the frequency shift will remain in the 10^{-17} range. The main difficulty is to determine the absolute value of the shift. The adiabatic passage technique is not implemented [10] which makes the evaluation more complex. We will study this effect during the 6 months ground tests. On ground, we can visualize the atomic distribution in the molasses to measure the initial atomic density as a function of the loading time or the laser intensities. With the detection of the time of flight, we can deduce the velocity distribution. From both measurements, the atomic cloud evolution inside the cesium tube is calculated. The cold collision shift is then simulated and the results are refined by experimental measurements. Furthermore, during the 18 months of the ACES mission, we will periodically measure this effect. By using the set of simulations and experimental results, we expect to get a relative frequency accuracy of 5 % of the collisional frequency shift. For atomic velocities of about 40 cm/s, the cold collision shift will be close to $1 \cdot 10^{-15}$.

The Ramsey cavity we have developed is a ring resonator. One coupling system feeds two symmetrical lateral waveguides which meet at the two interaction zones. Altogether, the cavity is made of 3 brazed copper pieces.

The master one includes the two interaction zones, the waveguides and, at the middle, the atom passage. A cap closes the master piece and the coupling is placed at the center (photo 1). The external dimensions are 298x100x46 mm. The advantage of this configuration is to provide large holes (8x9 mm) to let the atoms pass through with weak phase disturbances of the internal microwave field. As a precaution, at the input of the holes, a diaphragm reduces the aperture to limit atomic interactions with the cavity walls. A cavity prototype has been mounted inside the FO1 fountain [11], and no phase shift effects have been observed with a relative frequency resolution of 10^{-15} . Furthermore, we check the cavity symmetry with microwave measurements. These measurements are sensitive to a geometrical defect of few μ m. 4 microwave cavities have been constructed. By electrical measurements, we will select the better one. Then, this cavity will be mounted inside FO1 to study the phase shift effects before integration in the clock flight model. With the measurements and by simulations, we will be able to determine the cavity phase shift effect with an accuracy of 10^{-17} .

The clock performances evaluation will be made on ground and on board the space station. The duration will be 6 months for both. On ground, due to the gravity, the cesium tube will be vertical and the atoms will be launched upward or downward. The two configurations have to be studied to cancel systematic effects coming from the decelerating or accelerating movements of the atoms. As the duty cycle is low, the interrogation time is 100 ms, the quartz oscillator noise has a major contribution to the frequency stability of the clock. To circumvent this degradation, the quartz oscillator signal can be replaced by a cryogenic oscillator signal. The frequency stability of the clock will reach $2.5 \cdot 10^{-13} \tau^{-1/2}$ and a full accuracy evaluation at a level of 10^{-15} is then possible.

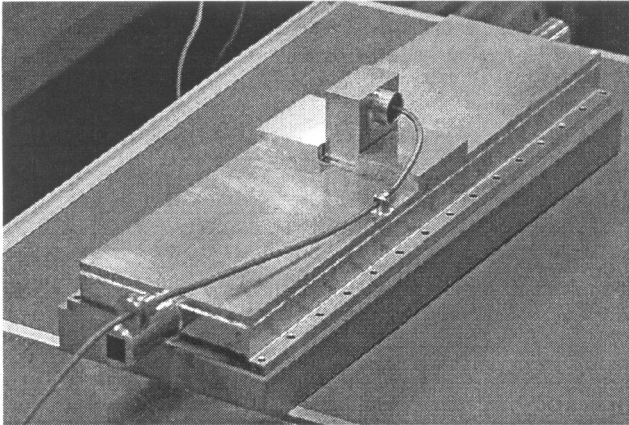


PHOTO1: A model of the Ramsey cavity. We can see, the cut-off wave-guide with a rectangular hole for the atomic paths and the central coupling. The cavity will be screwed on a rigid support to avoid plastic deformation of the copper.

By simulating the clock behavior in microgravity, we will be able to extrapolate these measurements to the 10^{-16} level

The ground support segment, in CNES, includes a maser, the mobile fountain FOM, a cryogenic oscillator from UWA, and a common-view GPS link with the BNM-SYRTE fountains in Paris. A vacuum chamber, with base plate temperature regulation, accommodates the Haraoh clock and the space H-maser provided by Observatoire de Neuchatel. The global performance of the clocks can be studied before assembly on the ACES payload.

IV. Clock sub-system description

Cesium tube

The cesium tube layout is shown in figure 6. The mass is 45 kg and the volume 70 liter. The cesium reservoir provides a cesium flux toward the capture region. The cesium flux is adjustable by varying the reservoir temperature or its aperture.

A valve is driven by a step by step motor. In the reservoir, a titanium matrix prevents migration of liquid cesium.

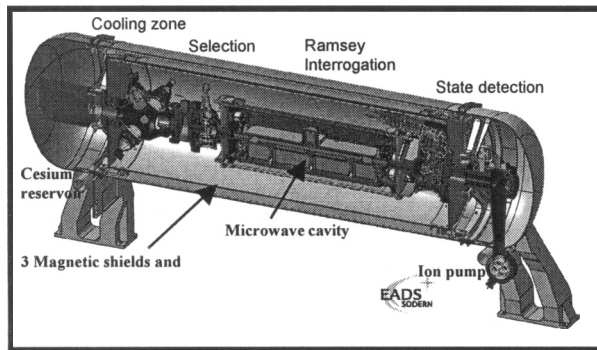


Fig. 6: Section of the cesium tube. (Courtesy of EADS SODERN).

The capture region includes the six collimators and 7 photodiodes for the measurements of the laser intensities and of the atomic fluorescence. A microwave cavity induces transition from the hyperfine level $F=4$ to the $F=3$. It is followed by two lasers beams to select the atoms in the $F=3$ level and eventually slice the atomic cloud by pushing away the $F=4$ atoms. 2 Photodiodes measure the laser power. Inside the interrogation region, the microwave cavity is screwed on a rigid mounting and some getters supply the necessary pumping rate. The detection region includes 4 tilted laser beams, 2 photodiodes for the laser power measurement and 2 temperature regulated photodiodes for the fluorescence detection. Finally, an ion pump provides the rare gas pumping.

Laser source

The layout of the laser source is shown in figure 7. It includes a double-side optical bench on which all optical components and the driving electronics are mounted. 4 extended cavity diode lasers supply high spectral quality beams. Two of them are for redundancy. A motor drives a half wave plate to switch from one ECDL to the other. Four diodes laser including two for redundancy are injected by one of the ECDL. They provide the capture laser beams. Six acousto-optic modulators allow tuning of the laser frequencies and control of the laser power. Seven mechanical shutters turn off the 10 useful laser beams sent to the cesium tube through optical fibers. To optimize coupling to the fibers, the laser beams alignment can be automatically adjusted by mirrors mounted on piezoelectric transducers.

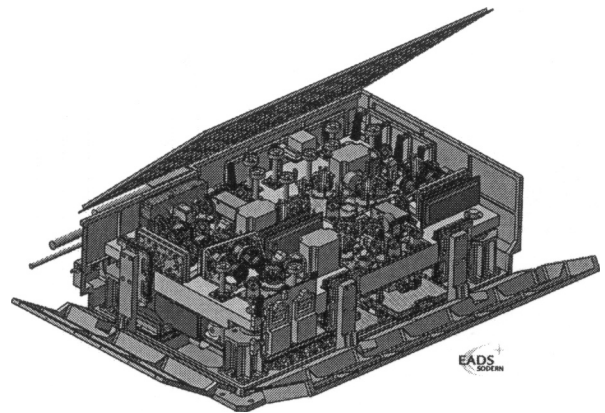


Fig. 7: Layout of the laser source. The double face optical bench is hold by 4 shock absorbers and thermally regulated. The electronic systems are fixed on the box base plate. (Courtesy of EADS SODERN).

Microwave source

The microwave source synthesizes, from a 5 MHz quartz oscillator, two 9.192... GHz signals and one 100 MHz signal. The 100 MHz and 9.192 GHz frequencies are finely tuned by two direct digital synthesizers. For Fourier frequencies below 100 Hz, the noise of these signals is dominated by the quartz

oscillator noise. The microwave output levels are controlled with a dynamic of 80 dB and can be switched off. In case of troubleshooting or during the ground tests, the 100 MHz stage can be switched off and replaced by an external signal.

Computer and software

The computer runs the real time software. It is linked to the clock sub-systems and to the ACES payload. It has a set of analog-digital converters to record nearly all physical signals, a digital bus to configure the sub-system parameters, to receive the remote controls and to send the clock measurements. It provides the digital pulses to trig all the phases of a clock cycle. The software manages the data communication, the servo-loops: sub-systems temperature regulations, microwave frequency servo-loop and magnetic field compensation, and the clock operation. Besides, it is able to control the ECDL operation, to automatically recover the optimum ECDL parameters and to lock the laser frequency. The software is easily configurable from the ground station.

V. Conclusion

All the clock sub-systems are designed and the critical elements are constructed and most are tested. By the way, we are able to predict the clock performances with confidence: the relative frequency stability will be $10^{-13} \tau^{-1/2}$ and the frequency accuracy will reach 10^{-16} . The accuracy budget will be mainly limited by the uncertainty on the collisional frequency shift.

From September 2004, the sub-systems of the engineering model will be delivered at CNES in Toulouse. The first systems are the computer and the microwave source. The laser source and the cesium tube will follow them. During 4 months, we will check all the functioning and the compatibility between the sub-systems. After that, the flight model construction will start. Then, 6 months will be necessary to evaluate the clock performances at a 10^{-15} level. A vacuum chamber with a thermal control has been constructed to simulate the ACES payload environment. It will receive the cold atom clock and the ACES H-maser.

VI. References

- [1] P. Laurent, G. Santarelli, S. Lea, S. Ghezali, M. Bahoura, E. Simon, A. Clairon, P. Lemonde, J. Reichel, A. Michaud, C. Salomon, "Cesium fountains and micro-gravity clocks," 25 th Moriond conference on Dark matter in cosmology, clocks and tests of fundamental laws, June 1995.
- [2] See, for instance, special issue of JOSA B6,1989.
- [3] Ph. Laurent, P. Lemonde, E. Simon, G. Santarelli, A. Clairon, N. Dimarcq, P. Petit, C. Audoin, and C. Salomon, "A cold atom clock in absence of gravity," *Eur. Phys. J. D*, vol. 3, pp. 201-204, (1998)
- [4] C. Salomon, P. Lemonde, P. Laurent, E. Simon, G. Santarelli, A. Clairon, P. Petit, N. Dimarcq, C. Audoin, F. Gonzalez, and F. Jamin Changeart, *Proc. of the 1st ESA symposium on Space Station Utilization*, SP385, 295 (1996).
- [5] Santarelli G., Laurent P., Lemonde P., Clairon, A., Mann A., Chang S., Luiten A., Salomon C., *Phys. Rev. Lett.* **82**, 4619-4622 (1999).

[6] G. Santarelli, C. Audoin, Ala Makdissi, Ph. Laurent, G.J. Dick and A. Clairon, « Frequency Stability Degradation of an Oscillator Slaved to a Periodically Interrogated Atomic Resonator », *IEEE Trans. Ultra. Ferr.*, vol. 45, n°4, 1998.

[7] See for instance the 1997 Nobel lectures: S. Chu, *Rev. Mod. Phys.*, **70**, 685 (1998); C. Cohen-Tannoudji, *ibid.*, p. 707; William D. Phillips, *ibid.*, p. 721.

[8] F. Allard, M. Abgrall, I. Maksimovic, Ph. Laurent, "an automatic system to control the operation of an extended cavity diode laser", to be published.

[9] E. Simon, P. Laurent, and A. Clairon, *Phys. Rev. A.*, vol. 57, P. 436, 1998.

[10] F. Pereira Dos Santos, H. Marion, S. Bize, Y. Sortais, A. Clairon, and C. Salomon, "Controlling the cold collision shift in high precision atomic interferometry", *Phys. Rev. Lett.* **89**, 233004 (2002)

[11] A. Clairon, P. Laurent, G. Santarelli, S. Ghezali, S.N. Lea, and M. Bahoura, "A cesium fountain frequency standard: preliminary results", *IEEE Transactions on Instrumentation and Measurement*, vol.44, N°2, avril 1995.